Entropy generation minimization of combined heat and mass transfer devices

Citation: Prakash Narayan, G., John H. Lienhard, and Syed M. Zubair. "Entropy Generation Minimization of Combined Heat and Mass Transfer Devices." International Journal of Thermal Sciences 49, no. 10 (October 2010): 2057–2066.

As Published: http://dx.doi.org/10.1016/j.ijthermalsci.2010.04.024

Publisher: Elsevier

Persistent URL: http://hdl.handle.net/1721.1/101904

Version: Author's final manuscript: final author's manuscript post peer review, without publisher's formatting or copy editing

Entropy Generation Minimization of Combined Heat and Mass Transfer Devices

G. Prakash Narayan[a], John H. Lienhard V[a,*], Syed M. Zubair[b]

[a]*Department of Mechanical Engineering, Massachusetts Institute of Technology, Cambridge, USA.*
[b]*Department of Mechanical Engineering, King Fahd University of Petroleum and Minerals, Dhahran, Saudi Arabia.*

Abstract

This paper details a simple procedure by which the entropy generation in simultaneous heat and mass exchange devices can be minimized. Effectiveness for these devices is defined and a new parameter, 'modified heat capacity rate ratio' is introduced. It is found that the entropy generation of a combined heat and mass exchange device is minimized (at constant value of effectiveness) when the modified heat capacity rate ratio is equal to one irrespective of the value of other independent parameters. Several typical examples of the cooling towers have been studied to illustrate this concept. A practical application of the concept is also illustrated using a humidification-dehumidification desalination system.

Keywords: Heat and mass exchangers, Entropy generation minimization, Humidification dehumidification desalination.

G.P. Narayan, J.H. Lienhard V, and S.M. Zubair, "Entropy Generation Minimization of Combined Heat and Mass Transfer Devices," International Journal of Thermal Sciences, 49(10):2057-2066, Oct. 2010.

*Corresponding author
Email address: lienhard@mit.edu (John H. Lienhard V)

Nomenclature

Symbols

c	Total molar concentration [mol/m^3]
$\dot{C}$	Heat capacity rate [W/K]
c_p	Specific heat capacity at constant pressure [J/kg·K]
D'	Thermal diffusion coefficient [m^2/s·K]
D_{AB}	Diffusion coefficient [m^2/s]
$\dot{H}$	Total enthalpy rate [W]
h	Specific enthalpy [J/kg]
h_a	Specific enthalpy of moist air [J/kg of dry air]
h_{fg}	Latent heat of evaporation [J/kg]
HCR	Heat capacity rate ratio [-]
k	Thermal conductivity [W/m·K]
$\dot{m}$	Mass flow rate [kg/s]
P	Absolute pressure [N/m^2]
$\dot{Q}$	Heat rate [W]
R	Gas constant [J/kg·K]
$\bar{R}$	Universal gas constant [J/mol·K]
s	Specific entropy [J/kg·K]
s_{fg}	Specific entropy change of evaporation [J/kg·K]
$\dot{S}_{gen}$	Entropy generation rate [W/K]
$\dot{S}'''_{gen}$	Entropy generation rate per unit volume[W/m^3·K]
T	Temperature [°C]
x	mass concentration [kg/kg]

Greek

Δ	Difference or change
ε	Component effectiveness [-]
ϕ	Relative humidity [-]
ω	Absolute humidity [kg/kg of dry air]
ρ	Density [kg/m^3]

Subscripts

a	Moist air
c	Cold stream
ct	Cooling tower or humidifier
da	Dehumidifier
da	Dry air
h	Hot stream
i	Inlet
max	Maximum
min	Minimum
o	Outlet
sat	Saturated

v	Vapor
w	Water

Superscripts

$ideal$	Ideal condition
mod	Modified

1. Introduction

Devices in which simultaneous heat and mass exchange occur are commonly used in the power and refrigeration industries. Cooling towers used in steam or combined cycle power plants are a typical example. Humidifiers and dehumidifiers used in HVAC systems are also examples. To optimize the performance of systems containing such devices, the irreversibilities of individual devices must be minimized [1, 2]. Since the total irreversibility of a system is the sum of the component irreversibilities, this procedure improves the system performance.

A few researchers [2-4] have previously attempted to optimize the second law design of heat and mass exchange devices by studying the sources of irreversibilities at the local level. Carrington and Sun [4] presented the following expression for the volumetric entropy generation rate as a sum of the three components that arise in combined heat and mass transfer processes. These include a mass transfer component, a heat transfer component and a coupled heat and mass transfer component, neglecting the irreversibilities due to fluid flow.

$$\dot{S}'''_{gen} = \frac{k}{T^2} \cdot (\nabla T)^2 + \frac{2\rho^2 \bar{R} D'}{M_A M_B c} (\nabla T) \cdot (\nabla x_A) + \frac{\rho^2 \bar{R} D_{AB}}{M_A M_B x_A x_B c} \cdot (\nabla x_A)^2 \qquad (1)$$

The first term on the right hand side of Eqn. 1 is the heat transfer component of the total irreversibility. In heat exchangers (without phase change or mass transfer, for example) this is the only term that causes the irreversibilities, other than the fluid flow irreversibilities. Hence, by balancing the stream-to-stream temperature difference in the heat exchangers we can minimize entropy production for a fixed effectiveness. In the following section it is shown how the temperature balance minimizes entropy production in a heat exchanger. However, the same is not true for a combined heat and mass exchange device, since in some situations the second and third term (related to mass diffusion irreversibilities) in Eqn. 1 can play a major role. Which component dominates the irreversibility depends on how steep the temperature and mass concentration gradients (x) are.

To exactly evaluate the contribution of each of the terms in Eqn. 1 on total irreversibility one has to perform a volume integral that requires knowledge of the local temperature and mass concentration profiles throughout the device. Hence, it is useful to apply a simple

control volume approach to identify the key variables governing the process. This paper develops a control volume procedure that facilitates minimization of the entropy generation in simultaneous heat and mass exchangers. The method uses an enthalpy-based effectiveness and modified heat capacity rate ratio, which is suitable for on-design analysis of adiabatic two-stream components within a cycle.

2. Heat exchangers

Several researchers have previously studied entropy production in heat exchangers [5-12]. In this section, we draw upon this literature to develop an understanding of how entropy production can be minimized for heat exchangers. Conservation equations for a counterflow heat exchanger shown in Fig. 1 are as follows. It is assumed that there is no phase change in either the hot or the cold fluid streams and that the heat exchanger has no heat loss to the environment.

Energy conservation is expressed by

$$\dot{m}_c \cdot (h_{2,c} - h_{1,c}) = \dot{m}_h \cdot (h_{2,h} - h_{1,h}) \tag{2}$$

and if the specific heat capacities are constant

$$\dot{m}_c c_{p,c} \cdot (T_{2,c} - T_{1,c}) = \dot{m}_h c_{p,h} \cdot (T_{2,h} - T_{1,h}) \tag{3}$$

Here, we have assumed that both the streams are incompressible and that the pressure change is negligible between the inlet and outlet. The Second Law gives,

$$\dot{S}_{gen} = \dot{m}_c \cdot (s_{2,c} - s_{1,c}) + \dot{m}_h \cdot (s_{1,h} - s_{2,h}) \tag{4}$$

$$= \dot{m}_c c_{p,c} \cdot \ln\left(\frac{T_{2,c}}{T_{1,c}}\right) + \dot{m}_h c_{p,h} \cdot \ln\left(\frac{T_{1,h}}{T_{2,h}}\right) \geq 0 \tag{5}$$

The heat exchanger effectiveness is defined in the usual fashion as actual to maximum heat transfer:

$$\varepsilon \equiv \frac{\dot{Q}}{\dot{Q}_{\max}} \tag{6}$$

$$\dot{Q}_{\max} = (\dot{m} \cdot c_p)_{\min} \cdot (T_{2,h} - T_{1,c}) \tag{7}$$

We define the heat capacity rate ratio (HCR) as

$$\text{HCR} \equiv \frac{\dot{m}_c \cdot c_{p,c}}{\dot{m}_h \cdot c_{p,h}} \equiv \frac{\dot{C}_c}{\dot{C}_h} \tag{8}$$

Using these equations we can write the entropy generation in two possible ways,

Case I, $\dot{C}_c < \dot{C}_h$:

$$\frac{\dot{S}_{gen}}{\dot{C}_c} = \frac{1}{\text{HCR}} \cdot \ln\left\{1 - \varepsilon \cdot \text{HCR}\left(1 - \frac{T_{1,c}}{T_{2,h}}\right)\right\} + \ln\left\{1 + \varepsilon\left(\frac{T_{2,h}}{T_{1,c}} - 1\right)\right\} \tag{9}$$

Case II, $\dot{C}_h < \dot{C}_c$:

$$\frac{\dot{S}_{gen}}{\dot{C}_h} = \text{HCR} \cdot \ln\left\{1 + \frac{1}{\text{HCR}}\varepsilon\left(\frac{T_{2,h}}{T_{1,c}} - 1\right)\right\} + \ln\left\{1 - \varepsilon\left(1 - \frac{T_{1,c}}{T_{2,h}}\right)\right\} \tag{10}$$

Hence, it can be seen that entropy production depends on these parameters:

$$\frac{\dot{S}_{gen}}{\dot{C}_{\min}} = f\left\{\left(\frac{T_{2,h}}{T_{1,c}} - 1\right), \text{HCR}, \varepsilon\right\} \tag{11}$$

In Fig. 2, we have shown that for various values of effectiveness and a fixed temperature ratio, the non-dimensional entropy generation is minimized at HCR=1. A simple calculation shows that this is true for all values of temperature ratio and effectiveness. At this condition, the heat exchanger is said to be 'balanced'. It is important to understand that the stream-to-stream temperature difference is constant throughout the length of the heat exchanger in this condition (see Eqn. 3 and 8). In other words, the driving force (temperature difference) is balanced.

3. Simultaneous heat and mass exchangers

The driving force for energy transfer in a combined heat and mass exchanger is a combination of both the temperature difference and the concentration difference. In this section, we take several typical examples for a cooling tower to explain how the entropy generation can be minimized by balancing this driving force. First, we define some new terminology

which is helpful in understanding these details.

3.1. Terminology used

The heat exchanger terminology that is used in the previous section is not directly applicable to combined heat and mass exchangers. For example, in a counterflow cooling tower (where hot water is losing heat and mass to humid air by direct contact), it is not possible to define the change in enthalpy of the moist air stream as the product of specific heat capacity at constant pressure and change in temperature because the humidity ratio should also be considered:

$$h_a = f\{T, P, \omega\} \tag{12}$$

If we neglect the effect of pressure variation on enthalpy

$$dh_a = c_{p,a} \cdot dT + \left(\frac{\partial h_a}{\partial \omega}\right)_{P,T} \cdot d\omega \tag{13}$$

where

$$c_{p,a} \equiv \left(\frac{\partial h_a}{\partial T}\right)_{P,\omega} \tag{14}$$

Alternatively, the enthalpy of moist air (air-water vapor mixture), can be defined as,

$$h_a - h_{ref} = c_{p,da} \cdot (T - T_{ref}) + \omega \cdot [c_{p,v} \cdot (T - T_{ref}) + h_{fg}] \tag{15}$$

In the above equation, it is assumed for purposes of discussion that the water vapor and dry air are ideal gases and also that their specific heat capacities are constant (in the calculations of Section 3.3, exact properties are used). Taking these ideas into consideration, we define the component effectiveness carefully before we look at examples of balancing the heat and mass exchanger.

3.1.1. Component effectiveness

An energy effectiveness (analogous to the effectiveness defined in heat exchanger design) is defined here. This definition is based on the maximum change in total enthalpy rate that can be achieved in an adiabatic heat and mass exchanger. Figure 3 illustrates the second law limitations imposed on a counterflow cooling tower. In the figure, 'wb,1' is the wet bulb point

of the air at the inlet to the humidifier and 'a,2' is the exit air state. The air is assumed to be saturated at the inlet and hence, $T_{wb,1} = T_{a,1}$. The saturation line connecting the point 'wb,1' to 'a,2' represents one possible process path for the humidification process. The maximum dry bulb temperature that can be achieved by the saturated air at the exit of the humidifier is the water inlet temperature (indicated by point 'a,3'). From Fig. 3, we see that the maximum possible change in enthalpy rate for saturated air entering the humidifier occurs if the air can be brought to saturation at the water inlet temperature ($\Delta\dot{H}_{max,a} = \dot{m}_{da} \cdot (h_{a,o}^{ideal} - h_{a,i})$). The required energy is drawn from the water stream, which may or may not have the capacity rate ($\dot{m}_w c_{p,w}$) necessary to supply that amount of energy within the limits imposed by the air and water inlet temperatures. If the water stream lacks sufficient capacity, the maximum possible change in total enthalpy rate will be that which cools the water to the air inlet temperature ($\Delta\dot{H}_{max,w} = \dot{m}_{w,i} \cdot h_{w,i} - \dot{m}_{w,o} \cdot h_{w,o}^{ideal}$). In this case the outlet air will be cooler than the water inlet temperature, and it may or may not be saturated.

Two parameters are required to fix the exit state of the air. In this analysis we fix the enthalpy and the relative humidity. The enthalpy is fixed indirectly by setting the effectiveness of the humidifier which is defined as the ratio of actual change in total enthalpy rate of either stream ($\Delta\dot{H}$) to maximum possible change in total enthalpy rate ($\Delta\dot{H}_{\max}$):

$$\varepsilon = \frac{\Delta\dot{H}}{\Delta\dot{H}_{\max}} \tag{16}$$

Based on this definition, ε may be written in terms of mass flow rates, temperatures, and the humidity ratio (see Fig. 4):

Case I, $\Delta\dot{H}_{max,w} < \Delta\dot{H}_{max,a}$;

$$\varepsilon = \frac{\dot{m}_{w,i} \cdot h_{w,i} - \dot{m}_{w,o} \cdot h_{w,o}}{\dot{m}_{w,i} \cdot h_{w,i} - \dot{m}_{w,o} \cdot h_{w,o}^{ideal}} \tag{17}$$

Case II, $\Delta\dot{H}_{max,w} > \Delta\dot{H}_{max,a}$;

$$\varepsilon = \frac{\dot{m}_{da} \cdot (h_{a,o} - h_{a,i})}{\dot{m}_{da} \cdot (h_{a,o}^{ideal} - h_{a,i})} \tag{18}$$

For a cooling tower, $h_{w,o}^{ideal}$ is the enthalpy of water at the inlet air temperature and $h_{a,o}^{ideal}$ is

the enthalpy of saturated moist air at inlet water temperature.

In addition to defining the effectiveness, we need to fix the exit relative humidity to completely specify the cooling tower performance. For any given case, a particular range of exit relative humidities are possible (corresponding to points from 'a,2' to 'a$'$, 2' shown in Fig. 3). Hence, the exit relative humidity is treated as a variable in this study.

The effectiveness of a cooling tower defined in this section varies from zero to a maximum value. The maximum value of the effectiveness is constrained by the Second Law and by the fact that the temperature of the air stream cannot exceed the temperature of the water stream at the hot end of the heat and mass exchanger. The latter is because it is not possible to have rate processes that will increase the temperature of air to above the temperature of water and also increase the humidity of the air stream at the same time. The maximum value depends on the inlet air and water temperatures, the inlet relative humidity, the operating pressure), the modified heat capacity ratio (HCR) (defined in section 3.1.3) and the exit air relative humidity.

An example of the variation of the maximum effectiveness with change in the exit relative humidity is shown in Fig. 5. The curves are plotted at various values of HCR. Each curve consists of two linear segments: 1. the horizontal segment at high relative humidities (> 0.9) and; 2. the sloped straight line at lower relative humidities. The first segment consists of data points that are constrainted by the Second Law ($\dot{S}_{gen} \geq 0; T_{a,i} < T_{w,i}$) and the second consists of points that are constrained by the temperature cross ($T_{a,i} \leq T_{w,i}; \dot{S}_{gen} > 0$). The second segment is linear because enthalpy varies linearly with relative humidity in the range of values we are interested in.

To incorporate the two constraints in the effectiveness definition, the maximum value of change in total enthalpy rate can be redefined as follows:

$$\Delta\dot{H}^{\text{mod}}_{\text{max}} = \varepsilon_{\text{max}} \cdot \min\left(\Delta\dot{H}_{\text{max},w}, \Delta\dot{H}_{\text{max},a}\right) \tag{19}$$

and Eqn. 16 would be modified by replacing $\Delta\dot{H}_{\text{max}}$ by $\Delta\dot{H}^{\text{mod}}_{\text{max}}$

This would ensure that the effectiveness varies from 0 to 1 (as for heat exchangers) and also that the $\dot{S}_{gen}$ will always be greater than 0 for $\varepsilon < 1$. However, this modification to the

definition of effectiveness will make it very cumbersome to evaluate a priori. Hence, we will use the definition in Eqn. 16.

3.1.2. Expression for entropy generation

Here we develop a similar expression for a heat and mass exchanger to identify the variables that affect $\dot{S}_{gen}$ in these devices. The example of a counterflow cooling tower (Fig. 4) is taken. An energy balance gives

$$\dot{m}_{w,i} \cdot h_{w,i} - \dot{m}_{w,o} \cdot h_{w,o} = \dot{m}_{da} \cdot (h_{a,o} - h_{a,i}) \tag{20}$$

Using Eqn. 15 we find the following expression for $T_{w,o}$:

$$\begin{aligned} T_{w,o} \;=\; & \left\{ \frac{\dot{m}_{w,i} \cdot c_{p,w}}{\dot{m}_{w,i} \cdot c_{p,w} - \dot{m}_{da} \cdot (\omega_o - \omega_i) \cdot c_{p,w}} \right\} T_{w,i} \\ & + \left\{ \frac{\dot{m}_{da} \cdot (c_{p,da} + c_{p,v} \cdot \omega_i)}{\dot{m}_{w,i} \cdot c_{p,w} - \dot{m}_{da} \cdot (\omega_o - \omega_i) \cdot c_{p,w}} \right\} T_{a,i} \\ & - \left\{ \frac{\dot{m}_{da} \cdot (c_{p,da} + c_{p,v} \cdot \omega_o)}{\dot{m}_{w,i} \cdot c_{p,w} - \dot{m}_{da} \cdot (\omega_o - \omega_i) \cdot c_{p,w}} \right\} T_{a,o} \\ & - \left\{ \frac{\dot{m}_{da} \cdot h_{fg,o}}{\dot{m}_{w,i} \cdot c_{p,w} - \dot{m}_{da} \cdot (\omega_o - \omega_i) \cdot c_{p,w}} \right\} \omega_o \\ & + \left\{ \frac{\dot{m}_{da} \cdot h_{fg,i}}{\dot{m}_{w,i} \cdot c_{p,w} - \dot{m}_{da} \cdot (\omega_o - \omega_i) \cdot c_{p,w}} \right\} \omega_i \end{aligned} \tag{21}$$

where, $h_{fg,o}$ and $h_{fg,i}$ are evaluated at the inlet and outlet air temperatures. From the definition of effectiveness, we have two cases.

Case I, $\Delta\dot{H}_{max,w} < \Delta\dot{H}_{max,a}$:

$$T_{w,o} = \left\{ \frac{\dot{m}_{w,i}}{\dot{m}_{w.i} - (\omega_o - \omega_i) \cdot \dot{m}_{da}} \right\} T_{w,i} \cdot (1 - \varepsilon) + \varepsilon \cdot T_{a,i} \tag{22}$$

Case II, $\Delta\dot{H}_{max,w} > \Delta\dot{H}_{max,a}$:

$$\begin{aligned} T_{a,o} = \quad & \left\{ \frac{c_{p,da} + c_{p,v} \cdot \omega_i}{c_{p,da} + c_{p,v} \cdot \omega_o} \right\} (1 - \varepsilon)\, T_{a,i} + \varepsilon \cdot T_{w,i} \\ & -(1 - \varepsilon) \cdot \left\{ \frac{(\omega_o \cdot h_{fg,o} - \omega_i \cdot h_{fg,i})}{c_{p,da} + c_{p,v} \cdot \omega_o} \right\} \end{aligned} \tag{23}$$

Applying the Second Law to the control volume, we can derive the following expression for entropy production in a cooling tower (see Appendix):

$$\begin{aligned}\frac{\dot{S}_{gen}}{\dot{m}_{w,i}\cdot c_{p,w}} &= \ln\left(\frac{T_{w,o}}{T_{w,i}}\right)+\frac{\dot{m}_{da}\cdot c_{p,da}}{\dot{m}_{w,i}\cdot c_{p,w}}\cdot\ln\left(\frac{T_{a,o}}{T_{a,i}}\right)\\ &+\frac{\dot{m}_{da}\cdot c_{p,v}}{\dot{m}_{w,i}\cdot c_{p,w}}\cdot\ln\left(\frac{T_{a,o}}{T_{a,i}}\right)^{\omega_i}-\frac{\dot{m}_{da}\cdot c_{p,v}}{\dot{m}_{w,i}\cdot c_{p,w}}\cdot\ln\left(\frac{T_{w,o}}{T_{a,o}}\right)^{\omega_o-\omega_i}\\ &+\frac{\dot{m}_{da}}{\dot{m}_{w,i}\cdot c_{p,w}}\cdot(\omega_o-\omega_i)\cdot s_{fg,o}\\ &+\frac{\dot{m}_{da}\cdot R_w}{\dot{m}_{w,i}\cdot c_{p,w}}\cdot\ln\left(\frac{P_{sat,w,o}}{P_{total}}\right)^{\omega_o-\omega_i}\\ &+\frac{\dot{m}_{da}\cdot R_{da}}{\dot{m}_{w,i}\cdot c_{p,w}}\cdot\ln\left(\frac{1+1.608\cdot\omega_o}{1+1.608\cdot\omega_i}\right)\\ &-\frac{\dot{m}_{da}\cdot R_w}{\dot{m}_{w,i}\cdot c_{p,w}}\cdot\omega_o\cdot\ln\left(1+\frac{1}{1.608\cdot\omega_o}\right)\\ &+\frac{\dot{m}_{da}\cdot R_w}{\dot{m}_{w,i}\cdot c_{p,w}}\cdot\omega_i\cdot\ln\left(1+\frac{1}{1.608\cdot\omega_i}\right)\end{aligned}\tag{24}$$

where P_{sat} is the saturation vapor pressure of water. Using Eqns. 21-24 we can see that entropy has the following functional form;

$$\frac{\dot{S}_{gen}}{\dot{m}_{w,i}\cdot c_{p,w}}=f_1\left\{\frac{T_{w,i}}{T_{a,i}},\phi_o,\phi_i,\varepsilon,R_1,R_2,R_3,R_4,\frac{\dot{m}_{da}}{\dot{m}_{w,i}},P^*\right\}\tag{25}$$

where: $R_1=\frac{\dot{m}_{da}\cdot c_{p,da}}{\dot{m}_{w,i}c_{p,w}}$; $R_2=\frac{\dot{m}_{da}R_{da}}{\dot{m}_{w,i}c_{p,w}}$; $R_3=\frac{\dot{m}_{da}R_w}{\dot{m}_{w,i}c_{p,w}}$; $R_4=\frac{\dot{m}_{da}c_{p,v}}{\dot{m}_{w,i}c_{p,w}}$; $P^*=\frac{P_{total}}{P_{sat,w,o}}$. Also, we can see that the parameters in Eqn. 25 have the following functional form:

$$R_1,R_2,R_3,R_4=f_2\left\{\frac{\dot{m}_{da}}{\dot{m}_{w,i}},\frac{c_{p,da}}{c_{p,w}},\frac{R_{da}}{c_{p,w}},\frac{R_w}{c_{p,w}},\frac{c_{p,v}}{c_{p,w}}\right\}\tag{26}$$

and

$$P^*=f_3\left\{P_{total},\frac{\dot{m}_{da}}{\dot{m}_{w,i}},T_{a,i},T_{w,i},\varepsilon,\phi_o,\phi_i\right\}\tag{27}$$

Therefore, we can write Eqn. (25) as,

$$\frac{\dot{S}_{gen}}{\dot{m}_{w,i}\cdot c_{p,w}}=f_4\left\{T_{w,i},T_{a,i},\phi_o,\phi_i,\varepsilon,\frac{\dot{m}_{da}}{\dot{m}_{w,i}},\frac{c_{p,da}}{c_{p,w}},\frac{R_{da}}{c_{p,w}},\frac{R_w}{c_{p,w}},\frac{c_{p,v}}{c_{p,w}},P_{total}\right\}\tag{28}$$

In Section 3.3, we show how the non-dimensional entropy production can be minimized using this understanding.

3.1.3. Modified heat capacity rate ratio

In this section, we define a new term for the heat and mass exchange devices which we will call the 'modified heat capacity rate ratio'. In heat exchangers we defined the heat capacity rate ratio as follows.

$$\mathrm{HCR}_{HE} = \frac{\dot{C}_c}{\dot{C}_h} \tag{29}$$

This can be rewritten as

$$\mathrm{HCR}_{HE} = \left(\frac{\Delta\dot{H}_{\max,c}}{\Delta\dot{H}_{\max,h}}\right) \tag{30}$$

since the maximum temperature difference in $\Delta\dot{H}_{\max,c}$ and $\Delta\dot{H}_{\max,h}$ is the same (i.e., $\Delta\dot{H}_{\max,k} = \dot{m}_k c_{p,k} \cdot (T_{h,i} - T_{c,i})$, where $k = c$ or h). Similarly, for an HME device, we define

$$\mathrm{HCR} = \left(\frac{\Delta\dot{H}_{\max,c}}{\Delta\dot{H}_{\max,h}}\right) \tag{31}$$

3.1.4. Non-dimensional entropy generation

For heat exchangers, we saw that a non-dimensional entropy generation term $\frac{\dot{S}_{gen}}{(\dot{m}\cdot c_p)_{\min}}$ appears in the derivation. Similarly, we define a non-dimensional term for heat and mass exchangers.

Case I, $\Delta\dot{H}_{max,w} < \Delta\dot{H}_{max,a}$;

$$\frac{\dot{S}_{gen}}{(\dot{m}\cdot c_p)_{\min}} = \frac{\dot{S}_{gen}}{\left(\widehat{\dot{m}_w}\cdot c_{p,w}\right)} \tag{32}$$

Case II, $\Delta\dot{H}_{max,w} > \Delta\dot{H}_{max,a}$;

$$\frac{\dot{S}_{gen}}{(\dot{m}\cdot c_p)_{\min}} = \frac{\dot{S}_{gen}}{\left(\widehat{\dot{m}_w}\cdot c_{p,w}\cdot \mathrm{HCR}_{ct}\right)} \tag{33}$$

where, $\widehat{\dot{m}_w}$ is the average mass flow rate of water through the cooling tower and the term $(\widehat{\dot{m}_w}\cdot c_{p,w})\cdot \mathrm{HCR}_{ct}$, which arises from Eqn. 33, can be thought of as an equivalent moist air

heat capacity. In this paper, $\widehat{\dot{m}_w}$ has been calculated as the average of the mass flow rates of water at the inlet and the outlet.

$$\widehat{\dot{m}_w} \approx \frac{\dot{m}_{w,i} + \dot{m}_{w,o}}{2} \tag{34}$$

The typical difference in water mass flow rate from inlet to outlet in a cooling tower is 5%. Hence, the inlet water mass flow can also be used as a good approximation to the average water mass flow for the cooling tower cases presented in this paper.

3.2. Solution technique

We have described the functional dependence of various parameters on entropy production by analytical expressions derived by making several simplifying approximations. Some of these such as the ideal gas approximation (Eqn. 15) introduce inaccuracies. Hence, all following simulations are performed using the commercial software, **Engineering Equation Solver (EES)** [13] which uses accurate equations of state to model the properties of moist air and water. Moist air properties are evaluated using the formulations presented by Hyland and Wexler [14], which are in close agreement with the data presented in ASHRAE Fundamentals [15]. EES calculates water properties using the IAPWS (International Association for Properties of Water and Steam) 1995 Formulation [16].

EES is a numerical solver, and it uses an iterative procedure to solve the equations. The convergence of the numerical solution is checked by using the following two variables: (1) 'Relative equation residual'- the difference between left-hand and right-hand sides of an equation divided by the magnitude of the left-hand side of the equation; and (2) 'Change in variables'- the change in the value of the variables within an iteration. The calculations converge if the relative equation residuals are less than 10^{-6} or if change in variables is less than 10^{-9}. These are default values in EES. There are several publications which have previously used EES for thermodynamic analysis [17-19].

The code written in EES was checked for correctness against various limiting cases. For example when $\varepsilon_{ct} = 0$, $\dot{S}_{gen}$ was found to be 0 for all values of input variables. When $\varepsilon_{ct} = 1$, the minimum stream-to-stream terminal (at exit or inlet) temperature difference in the cooling tower was identically equal to zero for all values of input variables. Several

other simple cases were checked. Also, calculations were repeated several times to check for consistency.

3.3. Results

3.3.1. Effect of mass flow rate ratio

In Section 3.1.2, we showed that the non-dimensional entropy generation of a cooling tower is a function of the inlet temperatures, the component effectiveness, the exit and inlet relative humidities, the ratio of certain specific heat capacities $\left(\frac{c_{p,da}}{c_{p,w}}, \frac{R_{da}}{c_{p,w}}, \frac{R_w}{c_{p,w}}, \frac{c_{p,v}}{c_{p,w}}\right)$, the absolute pressure and the mass flow rate ratio. Figure 6 illustrates the importance of this understanding. The mass flow rate ratio is plotted against the non-dimensional entropy generation term $\left(\frac{\dot{S}_{gen}}{(\dot{m}.c_p)_{\min}}\right)$ for various values of inlet water temperature ($T_{w,i}$) of 55°C to 70°C, an inlet air temperature ($T_{a,i}$) of 34°C, an exit relative humidity (ϕ_o) of 70%, an inlet relative humidity (ϕ_i) of 90% and an effectiveness (ε_{ct}) of 80%. It can be observed that the non-dimensional entropy generation is minimized at a particular value of mass flow rate ratio. This is found to be true for all values of input variables (inlet temperatures, inlet and exit reltive humidities and component effectiveness). Hence, we can conclude that at fixed inlet conditions the optimum point for non-dimensional entropy generation is dependent only on the mass flow rate ratio.

In certain cases (e.g, in Fig. 6 for $T_{w,i} = 70$°C) the minimum entropy generation point cannot be attained within the constraints ($\dot{S}_{gen} \geq 0; T_{w,i} \geq T_{a,o}$). Also, there are points of zero entropy generation at effectiveness less than 1. These correspond to points of maximum effectiveness (Fig. 5). As noted in Section 3.1.1, a modified effectiveness (See Eqn. 19 and 16) will have a value of 1 at these points.

3.3.2. Optimization using modified heat capacity ratio

The optimum point for non-dimensional entropy generation occurs at a particular value of mass flow rate ratio, but this value varies with change in input variables (inlet temperatures, inlet and exit relative humidities and component effectiveness). In this section, we normalize the optimum point by using the modified heat capacity rate ratio defined in Section 3.1.3. We also look at the effect that the different input variables have on the non-dimensional entropy generation.

Effect of water inlet temperature ($T_{w,i}$). Figure 7 shows the non-dimensional entropy production plotted against modified heat capacity rate ratio for various values of water inlet temperature at fixed values of $T_{a,i}, \phi_o, \phi_i$ and ε. For this figure, the mass flow rate ratio is varied from 1.2 to 29 to generate cases with HCR from 0.2 to 2.5. Two important observations can be made from this graph: (1) Irrespective of the value of $T_{w,i}$, non-dimensional entropy generation is minimized at HCR=1; (2) There is not a monotonic correlation between the non-dimensional entropy generation and the water inlet temperature. This trend is consistent for various (fixed) values of $T_{a,i}, \phi_o, \phi_i$ and ε.

Effect of air inlet temperature ($T_{a,i}$). Figure 8 illustrates the effect that the air inlet temperature has on non-dimensional entropy production. As was the case with the previous example, the entropy production is minimized at HCR=1 at all values of $T_{a,i}$. Also, it can be observed that the non-dimensional entropy production increases with decreasing air inlet temperature. This trend is for fixed values of $T_{w,i}, \phi_o, \phi_i$ and ε.

Effect of component effectiveness (ε). In Section 3.1.1 we had defined 'component effectiveness' for combined heat and mass exchangers. Figure 9 illustrates the effect of this parameter on entropy production. As in previous examples, the minimum entropy production rate is achieved at HCR=1 for all values of ε_{ct}. Also, as one would predict, a larger effectiveness (which usually translates into a larger heat exchanger size) yields a smaller entropy production than the cases with lesser effectiveness for the same boundary conditions.

Effect of exit relative humidity of the air (ϕ_o). We had noted in Section 3.1 that to completely balance a heat and mass exchange device we have to balance the driving force of energy transfer, which is a combination of the temperature and concentration difference. In cooling towers, this concentration difference is represented by the difference in relative humidity of the air stream (between inlet and outlet, for example). Figure 10 shows that cooling towers are balanced at HCR=1 for different values of exit relative humidity. It can also be observed that non-dimensional entropy production varies only slightly with ϕ_o (the curves are almost on top of each other). This is because the range of exit relative humidities possible for the presented case is small.

Effect of inlet relative humidity of the air (ϕ_i). Figure 11 illustrates the effect of inlet air relative humidity on the non-dimensional entropy production. As we had observed previously, the entropy production minimizes at HCR=1 irrespective of the value of the independent variables. Also the entropy production is inversely correlated with ϕ_i.

Effect of pressure drop. Figure 12 illustrates the effect of pressure drop on the non-dimensional entropy production. For this example, the air side pressure drops are taken to be varying from 0 to 10 kPa. The entropy production minimizes at HCR=1 irrespective of how large or small the pressure drop is. Also entropy production increases with increase in pressure drop.

From the various examples in this section, it is clear that a combined heat and mass exchanger is 'balanced' and the entropy production is minimum when the modified heat capacity rate ratio is 1. Also, the functional dependence of the non-dimensional entropy production is

$$\frac{\dot{S}_{gen}}{(\dot{m}\cdot c_p)_{\min}} = f_5\left\{T_{w,i}, T_{a,i}, \phi_o, \phi_i, \varepsilon, \mathrm{HCR}, \frac{c_{p,da}}{c_{p,w}}, \frac{R_{da}}{c_{p,w}}, \frac{R_w}{c_{p,w}}, \frac{c_{p,v}}{c_{p,w}}, P_{total}\right\} \tag{35}$$

where

$$\mathrm{HCR} = \left(\frac{\Delta\dot{H}_{max,c}}{\Delta\dot{H}_{max,h}}\right) \tag{36}$$

4. Application in thermal design of a desalination system

In this section, we look to use the concept of 'balancing' combined heat and mass exchangers in a practical application. Figure 13 is a schematic diagram of a simple desalination system called the humidification-dehumidification (HDH) desalination system [20-22]. This system consists of two simultaneous heat and mass exchangers: (1) A humidifier which is similar to a cooling tower (an air stream gains heat and mass from direct contact with hot seawater stream in the humidifier); and (2) a dehumidifier which uses cold seawater to dehumidify the moist air stream to produce fresh water as condensate. Energy is input in a moist air heater which heats the moist air from the humidifier before it enters the dehumidifier.

For the HDH systems, a performance ratio called the gained-output-ratio (GOR) is commonly used. GOR is the ratio of the latent heat of evaporation of the distillate produced to

the total heat input absorbed by the moist air heater.

$$\mathrm{GOR} = \frac{\dot{m}_{pw} \cdot h_{fg}}{\dot{Q}_{in}} \tag{37}$$

This parameter is, essentially, the effectiveness of water production and an index of the amount of the heat recovery effected in the system. We will balance the humidifier and the dehumidifier by adjusting the modified heat capacity rate ratio (HCR) for these components, so as to improve the GOR of the system.

Figure 13 shows an example of the values of the different design parameters in the system. A component effectiveness of 90% is used for both the humidifier and the dehumidifier. A top temperature ($T_{a,3}$) of 90°C and a bottom temperature ($T_{w,0}$) of 30°C are used for design of this system. The feed seawater flow rate is 0.15 kg/s and the air flow through the system is 0.1 kg of dry air/s. For these conditions, the modified heat capacity rate ratios of the humidifier and the dehumidifier are 2.16 and 1.65 respectively. The GOR for the system shown is 2.9.

In Fig. 14, we have shown a possible configuration to bring the dehumidifier closer to a balanced condition. An extraction of air (at a temperature $T_{a,4}$) is made from the humidifier and it is injected in the dehumidifier (at a temperature $T_{a,5}$). The extracted mass flow ($\dot{m}_{a,ex}$) is 0.033 kg/s (33%). This divides the dehumidifier and the humidifier into two parts with different mass flow rate ratios (of 1.5 and 1.09). This causes the overall HCR of the dehumidifier to be brought closer to 1 (≈ 1.47) while that of the humidifier moves away from the balanced condition (≈ 2.61). All boundary conditions are as in Fig. 13. The overall entropy produced for the system is reduced, and the GOR increases to 3.35 (16% increase). Further, we can make multiple extractions of moist air from the humidifier and inject it in the dehumidifier to fully balance (HCR = 1) the dehumidifier.

In Fig. 15, a configuration to balance the humidifier in the same system is shown. Here, the direction of extraction is reversed. Thirty-one percent of humid air stream is extracted from the dehumidifier (at a temperature $T_{a,4}$) to the humidifier (at a temperature $T_{a,5}$). This brings the HCR of the humidifier closer to 1 (≈ 1.919) while that of the dehumidifier moves away from the balanced condition (HCR ≈ 1.912). Because the dehumidifier performance

dominates the system performance, the GOR of the system is reduced to 2.25. However, it can be seen that the humidifier can be fully balanced by making the system a multi-extraction system.

Müller-Holst [23] developed a similiar system without this theoretical framework. His scheme of extractions was aimed at minimizing the maximum stream-to-stream temperature difference. However, the minimum entropy generation is at a point where HCR =1, which is not the same as a situation in which temperature differences are balanced.

5. Conclusions

A comprehensive study to understand and optimize the Second Law performance of combined heat and mass exchange devices has been carried out. The following significant conclusions are arrived at from this study:

1. The entropy production can be usefully non-dimensionalized by dividing it by the heat capacity rate of the minimum heat capacity stream in the heat and mass exchanger $\left(\frac{\dot{S}_{gen}}{(\dot{m}\cdot c_p)_{\min}}\right)$.
2. A modified heat capacity rate ratio (HCR) for simultaneous heat and mass exchangers was defined as the ratio of the maximum possible change in total enthalpy rate of the cold stream to the maximum possible change in total enthalpy rate of the hot stream $\left(\text{HCR} = \frac{\Delta \dot{H}_{max,c}}{\Delta \dot{H}_{max,h}}\right)$.
3. The non-dimensional entropy production for a cooling tower is dependent on the following variables:
$$\frac{\dot{S}_{gen}}{(\dot{m}\cdot c_p)_{\min}} = f\left\{T_{w,i}, T_{a,i}, \phi_o, \phi_i, \varepsilon, \text{HCR}, \frac{c_{p,da}}{c_{p,w}}, \frac{R_{da}}{c_{p,w}}, \frac{R_w}{c_{p,w}}, \frac{c_{p,v}}{c_{p,w}}, P_{total}\right\}$$
It is noted that this includes performance parameters (ε, ϕ_o), inlet variables ($T_{w,i}$, $T_{a,i}$, $\frac{\dot{m}_{w,i}}{\dot{m}_{da}}$), pressure ($P_{total}$) and fluid properties ($c_{p,da}, c_{p,w}, c_{p,v}$, R_{da}, R_w). Operationally, HCR can be varied by only changing the mass flow rate ratio $\left(\frac{\dot{m}_{w,i}}{\dot{m}_{da}}\right)$. The component effectiveness contains the effects of the exchanger dimensions and material properties and is varied in an on-design sense.
4. The non-dimensional entropy production is minimized and the heat and mass exchanger is 'balanced' at HCR=1.

5. A typical desalination system was taken as an example of the practical application of the entropy minimization concept in thermal design of cycles that include simultaneous heat and mass exchangers.

Acknowledgments

The authors would like to thank the King Fahd University of Petroleum and Minerals for funding the research reported in this paper through the Center for Clean Water and Clean Energy at MIT and KFUPM.

References

[1] Kilic, M., Kaynakli, O., 2007. Second law-based thermodynamic analysis of water-lithium bromide absorption refrigeration system. *Energy* **32**(8), 1505-1512.

[2] Bejan, A., 1987. The thermodynamic design of heat and mass transfer processes and devices. *International Journal of Heat and Fluid Flow* **8**(4), 258-276.

[3] San, J.Y., Worek, W.M., Lavan, Z., 1987. Entropy generation in combined heat and mass transfer. *International Journal of Heat and Mass Transfer* **30**, 1359-68.

[4] Carrington, C.G., and Sun, Z.F., 1991 Second law analysis of combined heat and mass transfer phenomena. *International Journal of Heat and Mass Transfer* **34**(11), 2767-2773.

[5] Hesselgreaves, J.E., 2000. Rationalisation of second law analysis of heat exchangers. *International Journal of Heat and Mass Transfer* **43**, 4189-4204.

[6] Witte, L.C., Shamsundar, N., 1983. A thermodynamic efficiency concept for heat exchange devices. *Journal of Engineering for Power* **105**, 199-203.

[7] London, A.L., Shah R.K., 1983. Costs of irreversibilities in heat exchanger design. *Heat Transfer Engineering* **4**, 59-73.

[8] Sarangi, S., Choowdhury K., 1982. On the generation of entropy in a counterflow heat exchanger. *Cryogenics* **22**, 63-65.

[9] Sekulic, D.P., Entropy generation in a heat exchanger, 1986. *Heat Transfer Engineering* **7**, 83-88.

[10] Sciubba, E., 1996. A minimum entropy generation procedure for the discerte pseudo-optimization of finned-tube heat exchangers. *Revue Générale de Thermique* **35**, 517-525.

[11] Cornelissen, R.L., Hirs, G.G., 1999. Thermodynamic optimization of a heat exchanger. *International Journal of Heat and Mass Transfer* **42**, 951-959.

[12] Yilmaz, M., Saraa, S., Karsli, B., 2001. Performance evaluation criteria for heat exchangers based on second law analysis. *Exergy International Journal* **1**(4), 278-294.

[13] Klein, S.A. Engineering Equation Solver. Academic Professional, Version 8. URL http://www.fchart.com/ees/ees.shtml

[14] Hyland, R. W., Wexler, A., 1983. Formulations for the Thermodynamic Properties of the Saturated Phases of H2O from 173.15 K to 473.15 K. *ASHRAE Transactions* Part 2A, Paper 2793.

[15] Wessel, D.J., 2001. ASHRAE Fundamentals Handbook 2001 (SI Edition). *American Society of Heating, Refrigerating, and Air-Conditioning Engineers*.

[16] Pruss, A. and Wagner, W., 2002. The IAPWS formulation 1995 for the thermodynamic properties of ordinary water substance for general and scientific use. *Journal of Physical and Chemical Reference Data* **31**(2), 387-535.

[17] Pridasawas, W. and Lundqvist, P., 2007. A year-round dynamic simulation of a solar-driven ejector refrigeration system with iso-butane as a refrigerant. *International Journal of Refrigeration* **30**(5), 840-850.

[18] Zmeureanu, R. and Wu, X.Y, 2007. Energy and exergy performance of residential heating systems with separate mechanical ventilation. *Energy* **32**(3), 187-195.

[19] Qureshi, B.A. and Zubair, S.M., 2002. A complete model of wet cooling towers with fouling in fills. *Applied Thermal Engineering* **26**(16), 1982-1989.

[20] Narayan, G.P., Sharqawy, M.H., Summers, E.K., Lienhard V, J.H., Zubair, S.M. and Antar, M.A., 2010. The potential of solar-driven humidification-dehumidification desalination for small-scale decentralized water production, *Renewable and Sustainable Energy Reviews*, Volume 14, Issue 4, pp 1187-1201.

[21] Narayan, G.P., Sharqawy, M.H., Lienhard V, J.H., and Zubair, S.M., 2010. Thermodynamic analysis of humidification dehumidification desalination cycles, *Desalination and Water Treatment*, Vol 16, pp. 339-353.

[22] Mistry, K.H., Lienhard V, J.H., and Zubair, S.M., 2009. Second Law Analysis of Humidification-Dehumidification Desalination Cycles, Submitted for publication to *International Journal of Thermal Sciences*.

[23] Müller-Holst, H., 2007. Solar Thermal Desalination using the Multiple Effect Humidification (MEH) Method, in *Solar Desalination for the 21st Century*, Springer, Dordrecht.

List of figures

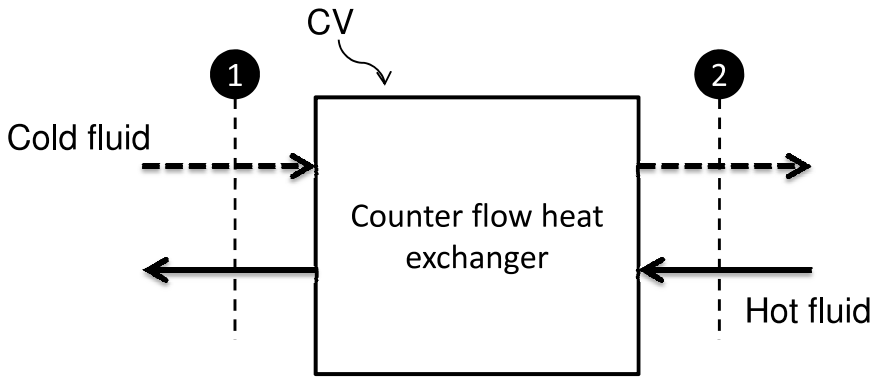

Figure 1: Control volume for a counter flow heat exchanger.

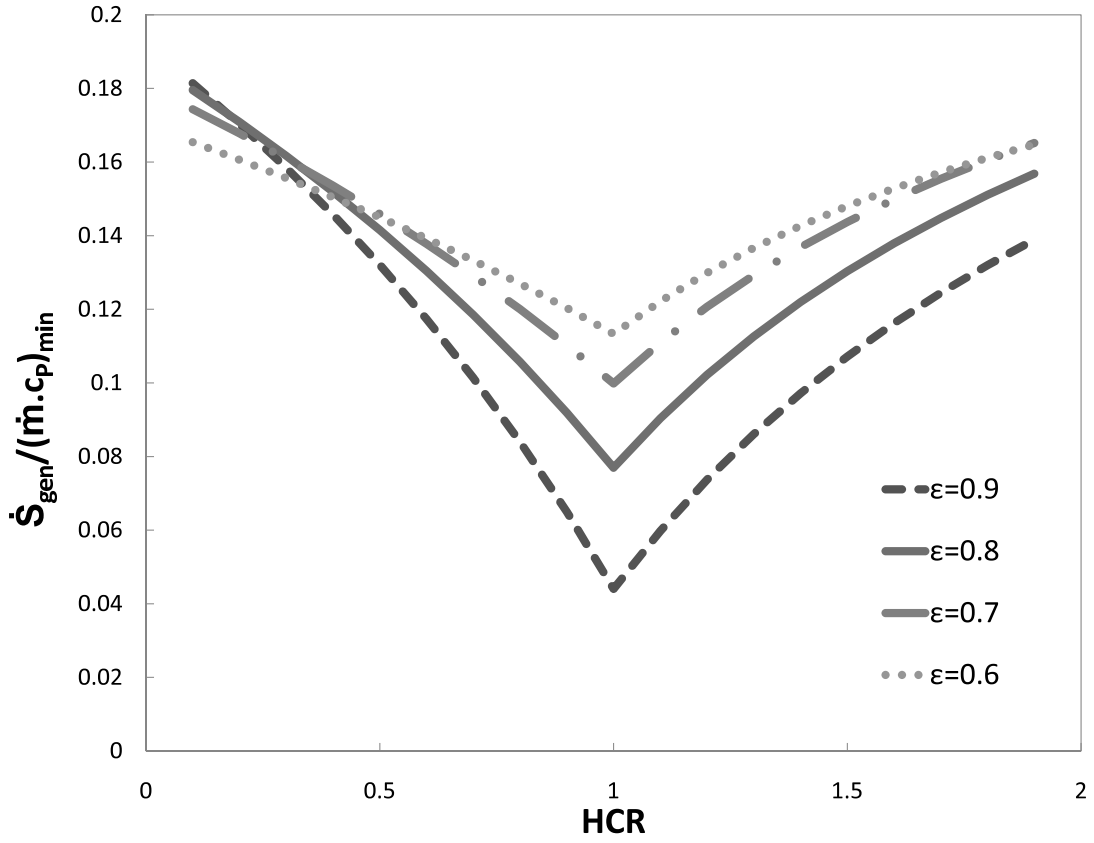

Figure 2: Non-dimensional entropy generation versus heat capacity rate ratio for counterflow heat exchangers; $\frac{T_{2,h}}{T_{1,c}} - 1 = 0.5$.

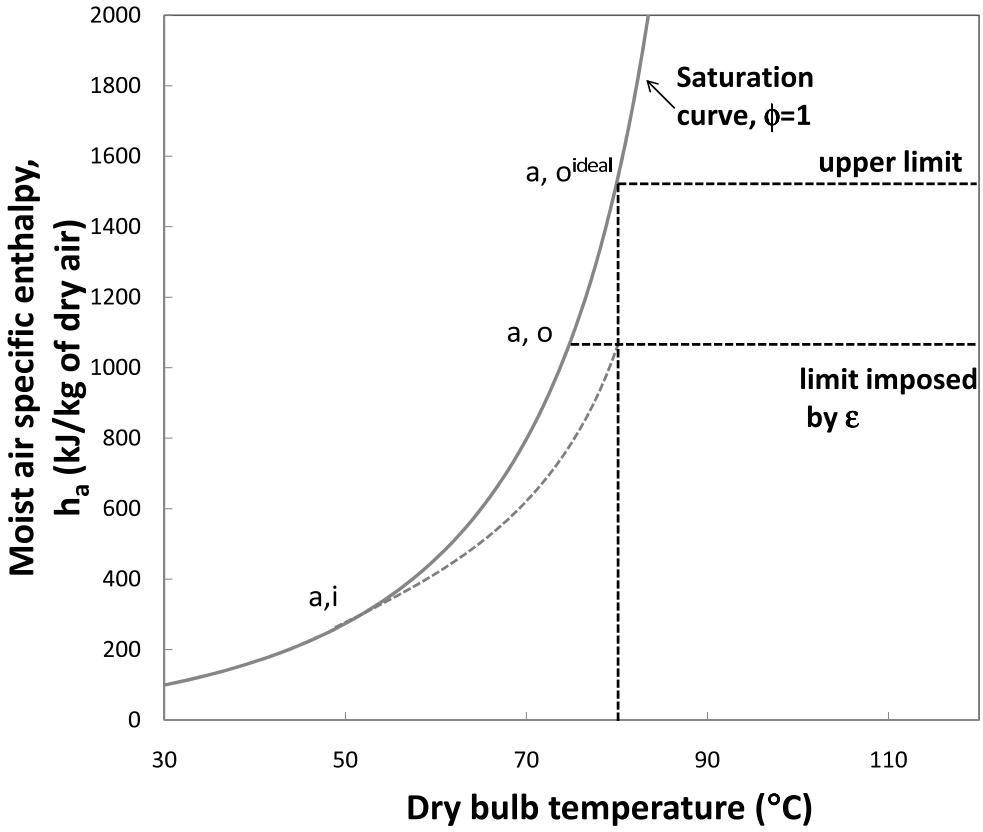

Figure 3: Psychometric chart (at P=1 atm) indicating the second law limits of energy transfer in a cooling tower.

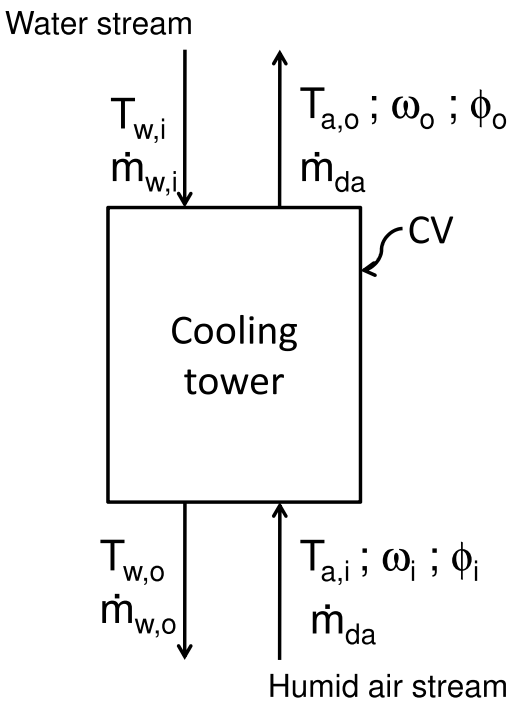

Figure 4: Control volume for a cooling tower.

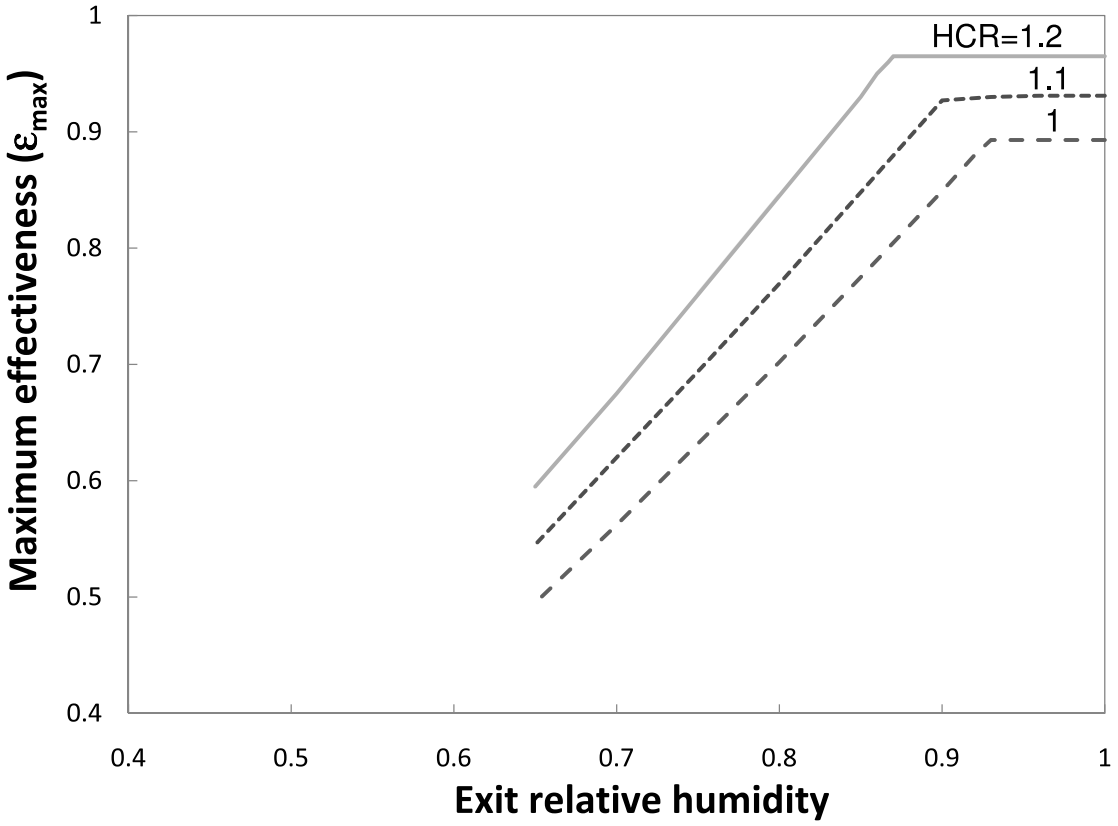

Figure 5: Maximum value of effectiveness versus exit relative humidity for a cooling tower; $T_{w,i} = 55°\text{C}; T_{a,i} = 34°\text{C}; \phi_{\text{i}} = 100\%; P = 100$ kPa.

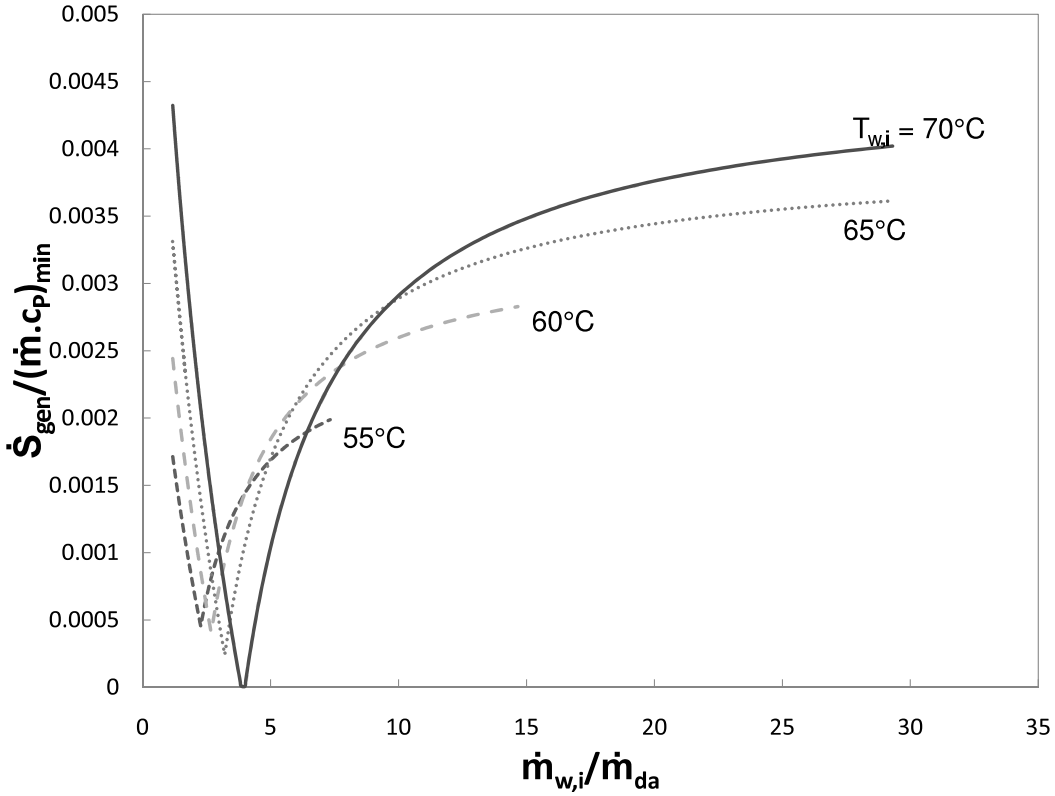

Figure 6: Effect of water inlet temperature on entropy generation in a cooling tower; $T_{a,i} = 34°\text{C}; \varepsilon_{ct} = 80\%; \phi_o = 90\%; \phi_i = 60\%; \frac{\dot{m}_{w,i}}{\dot{m}_{da}} = 1.2 - 29; P = 100$ kPa.

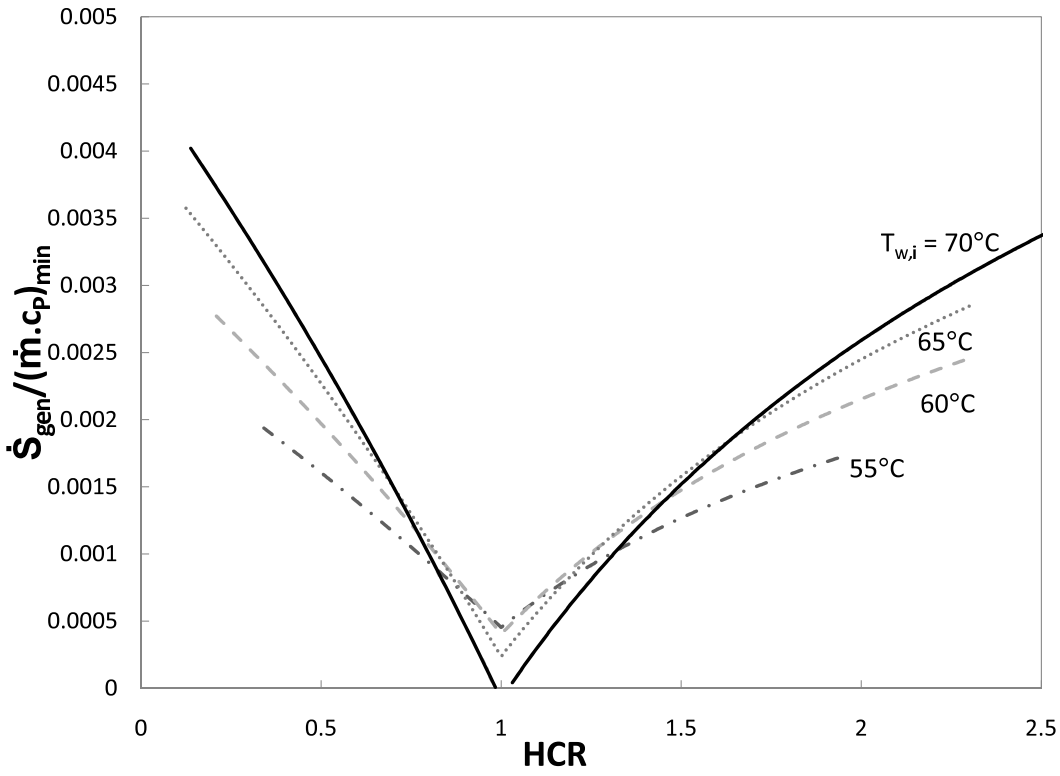

Figure 7: Mass flow rate ratio versus non-dimensional entropy generation; $T_{a,i} = 34°\text{C}; \varepsilon_{\text{ct}} = 80\%; \phi_{\text{o}} = 90\%; \phi_{\text{i}} = 60\%; P = 100$ kPa.

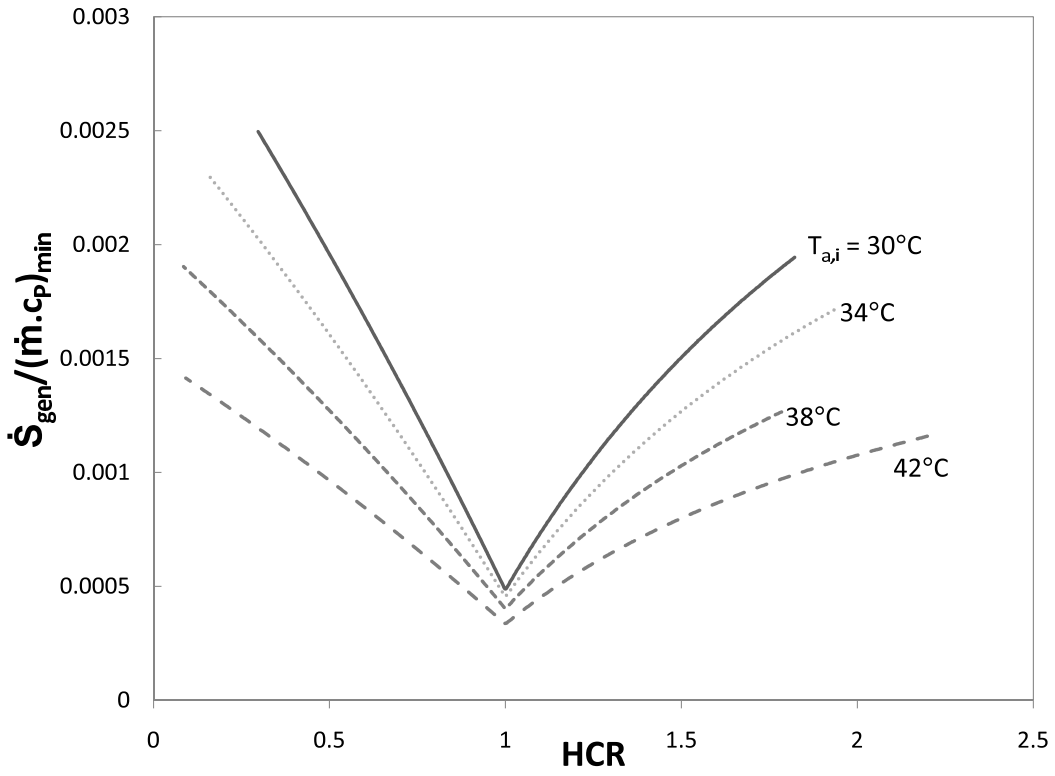

Figure 8: Effect of air inlet temperature on entropy generation in a cooling tower; $T_{w,i} = 55°\text{C}; \varepsilon_{ct} = 80\%; \phi_o = 60\%; \phi_i = 80\%; \frac{\dot{m}_{w,i}}{\dot{m}_{da}} = 1.2 - 29; P = 100$ kPa.

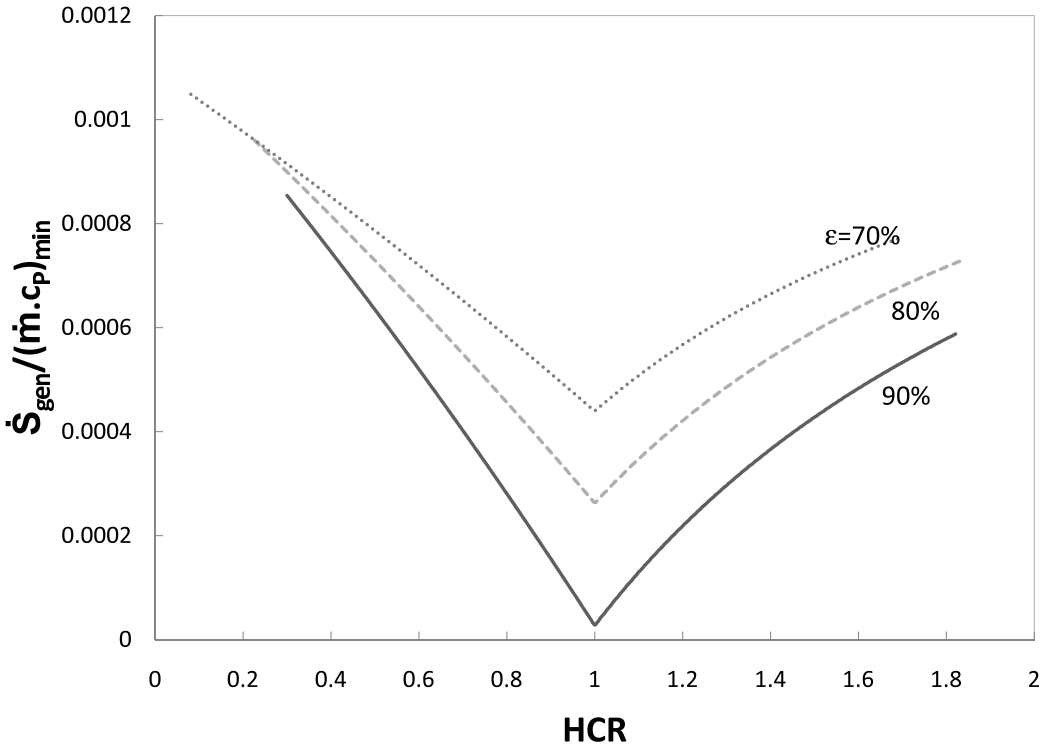

Figure 9: Effect of cooling tower effectiveness on entropy generation;$T_{w,i} = 55°\text{C}; T_{a,i} = 34°\text{C}; \phi_o = 90\%; \phi_i = 60\%; \frac{\dot{m}_{w,i}}{\dot{m}_{da}} = 1.2 - 29; P = 100$ kPa.

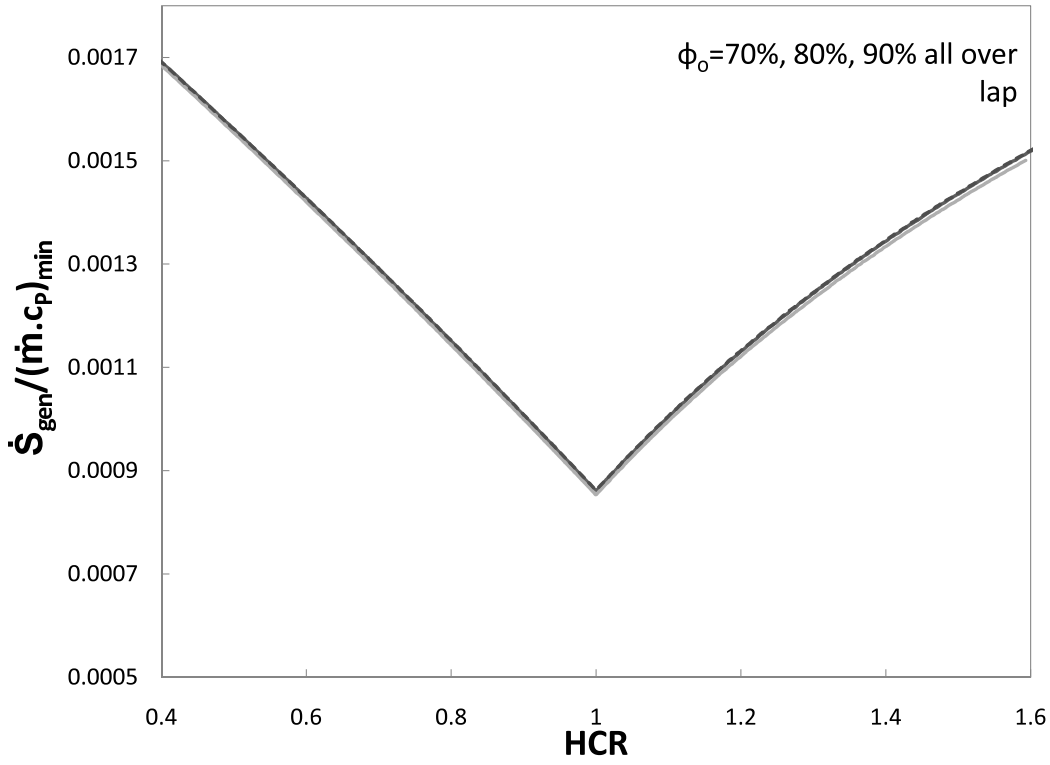

Figure 10: Effect of outlet air relative humidity on entropy generation in a cooling tower; $T_{w,i} = 50°\text{C}; T_{a,i} = 34°\text{C}; \varepsilon_{ct} = 70\%; \phi_i = 50\%; \frac{\dot{m}_{w,i}}{\dot{m}_{da}} = 1.2 - 29; P = 100$ kPa.

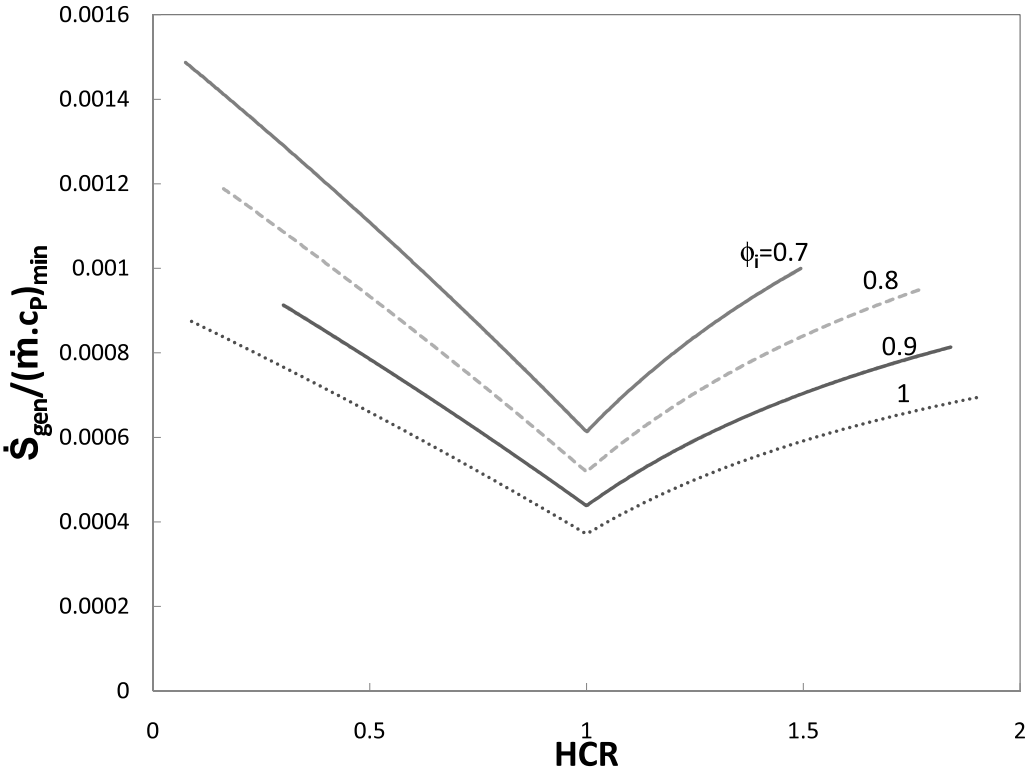

Figure 11: Effect of inlet air relative humidity on entropy generation in a cooling tower; $T_{w,i} = 50°\text{C}; T_{a,i} = 34°\text{C}; \varepsilon_{ct} = 70\%; \phi_o = 90\%; \frac{\dot{m}_{w,i}}{\dot{m}_{da}} = 1.2 - 29; P = 100$ kPa.

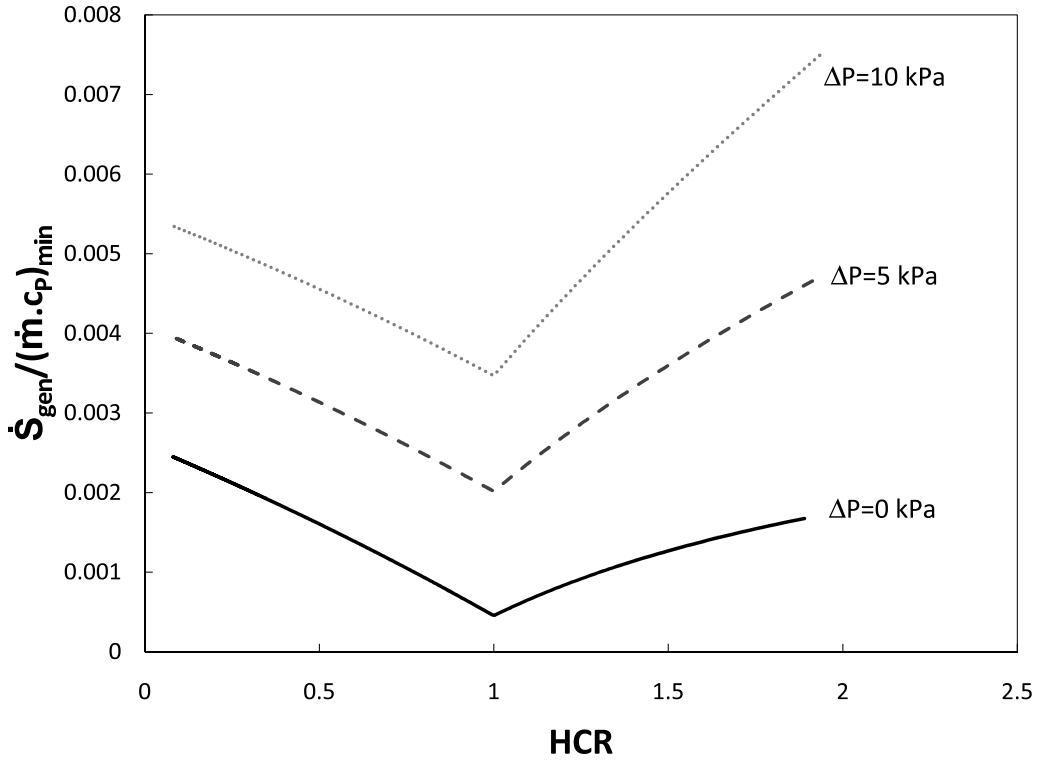

Figure 12: Effect of pressure drop on entropy generation in a cooling tower; $T_{w,i} = 55°\text{C}; T_{a,i} = 34°\text{C}; \varepsilon_{ct} = 80\%; \phi_o = 90\%; \phi_i = 60\%; \frac{\dot{m}_{w,i}}{\dot{m}_{da}} = 1.2 - 29; P_{a,o} = 100$ kPa.

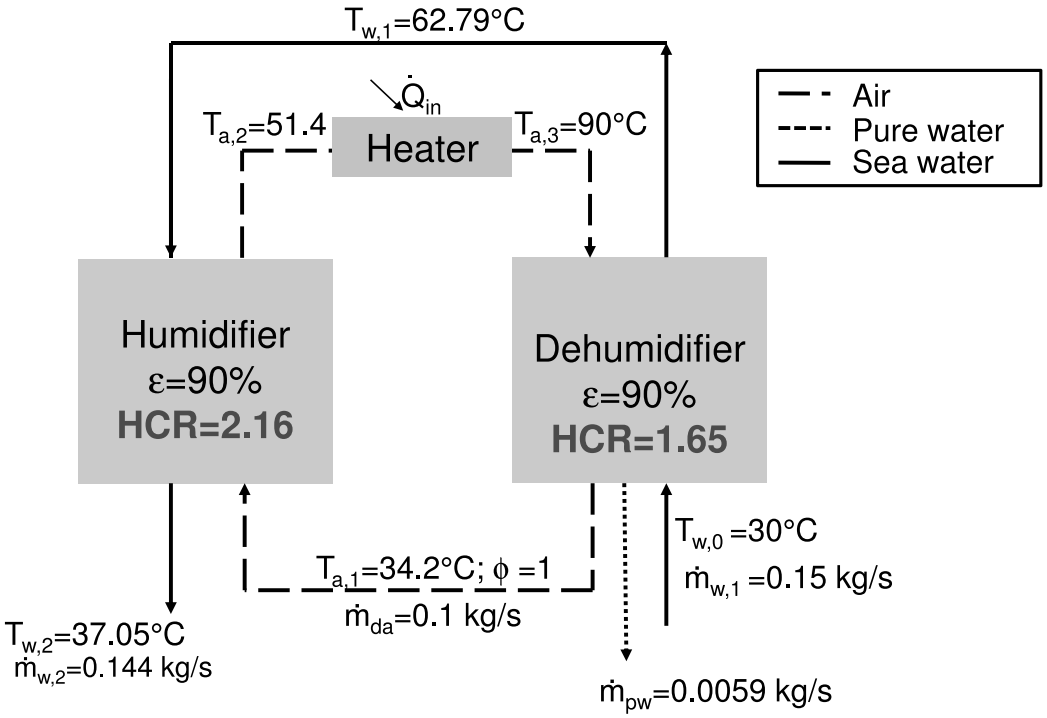

Figure 13: A schematic diagram of the air-heated humidification dehumidification desalination system.

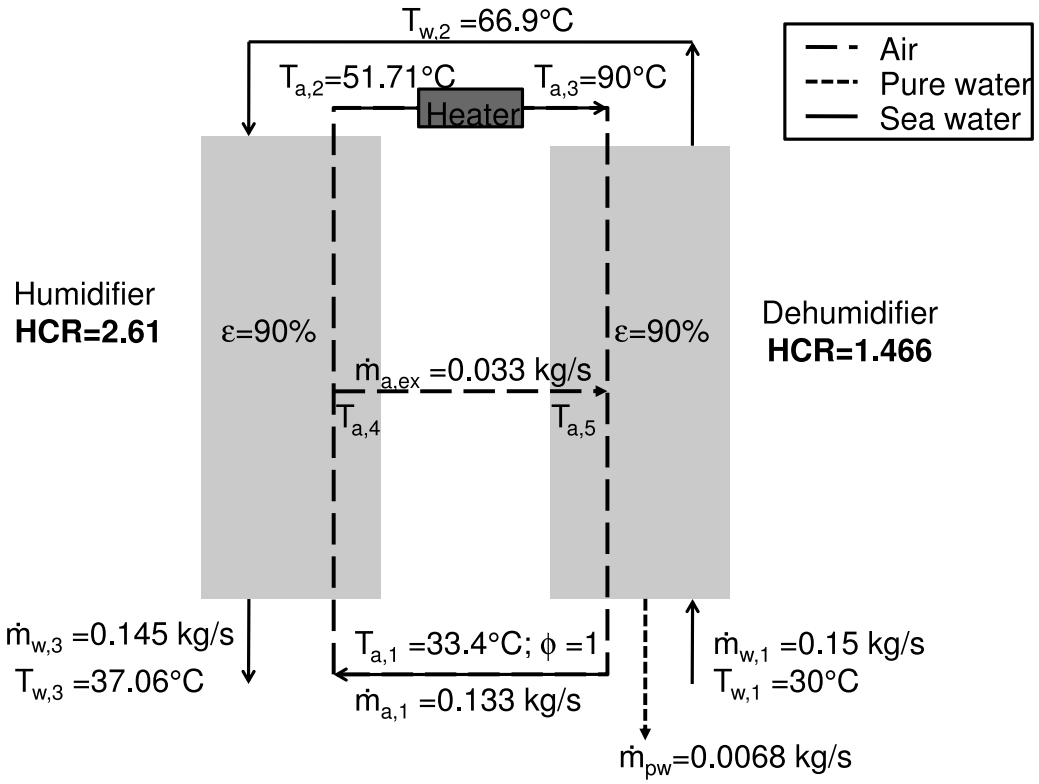

Figure 14: A schematic diagram of the air-heated humidification dehumidification desalination system with a single extraction of the air stream to balance the dehumidifier.

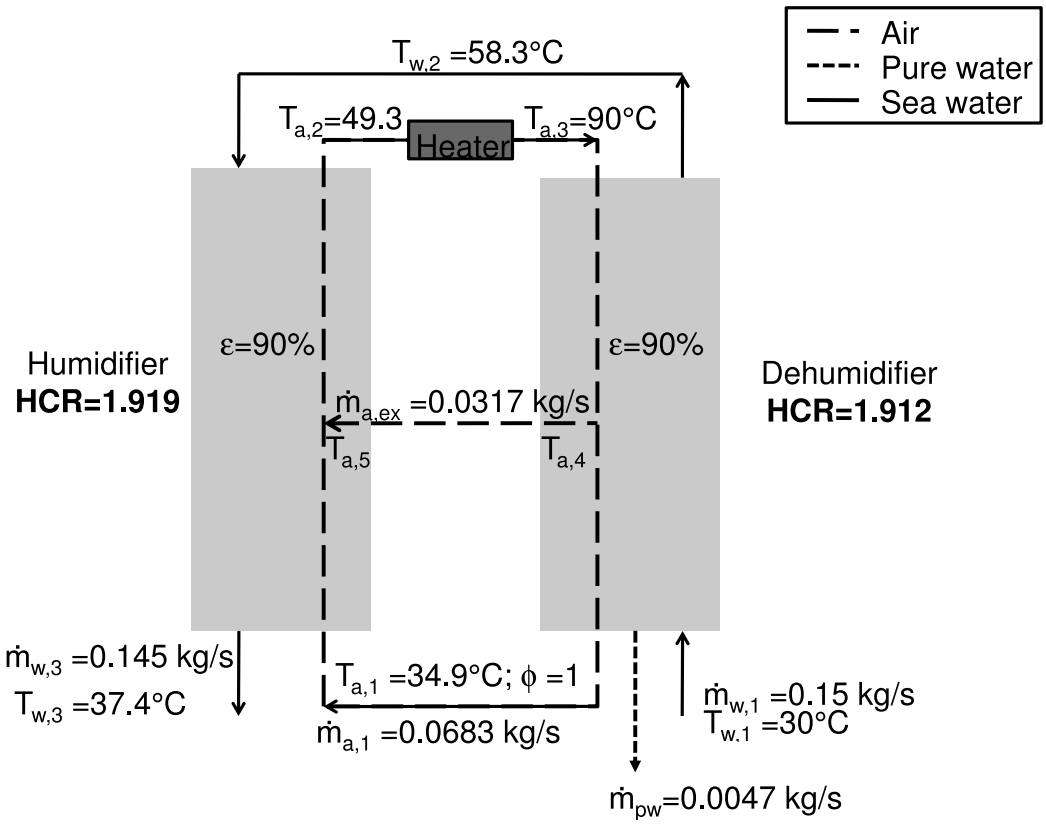

Figure 15: A schematic diagram of the air-heated humidification dehumidification desalination system with a single extraction of the air stream to balance the humidifier.

Appendix A. Entropy generation in a counterflow cooling tower

Using the control volume in Fig. 5,

$$\dot{S}_o = \dot{m}_{w,o} \cdot s_{w,o} + \dot{m}_{a,o} \cdot s_{a,o} \tag{A.1}$$

$$\dot{S}_i = \dot{m}_{w,i} \cdot s_{w,i} + \dot{m}_{a,i} \cdot s_{a,i} \tag{A.2}$$

Applying the Second Law to the same isolated control volume,

$$\dot{S}_{gen} = \dot{S}_o - \dot{S}_i \tag{A.3}$$

$$\begin{aligned} &= \dot{m}_{w,i} \cdot (s_{w,o} - s_{w,i}) - (\dot{m}_{w,i} - \dot{m}_{w,o}) \cdot s_{w,o} \\ &\quad + \dot{m}_{a,o} \cdot s_{a,o} - \dot{m}_{a,i} \cdot s_{a,i} \geq 0 \end{aligned} \tag{A.4}$$

Moist air entropy can be written as:

$$\dot{m}_{a,o} \cdot s_{a,o} = \dot{m}_{da} \cdot s_{da,o} + \dot{m}_{da} \cdot \omega_o \cdot s_{v,o} \tag{A.5}$$

$$\dot{m}_{a,i} \cdot s_{a,i} = \dot{m}_{da} \cdot s_{da,i} + \dot{m}_{da} \cdot \omega_i \cdot s_{v,i} \tag{A.6}$$

Now Eqn. A.4 can be written as:

$$\begin{aligned} \dot{S}_{gen} &= \dot{m}_{w,i} \cdot (s_{w,o} - s_{w,i}) - (\dot{m}_{w,i} - \dot{m}_{w,o}) \cdot s_{w,o} \\ &\quad + \dot{m}_{da} \cdot (s_{da,o} - s_{da,i}) + \dot{m}_{da} \cdot \omega_i \cdot (s_{v,o} - s_{v,i}) \\ &\quad + \dot{m}_{da} \cdot (\omega_o - \omega_i) \cdot s_{v,o} + \Delta\dot{S}_{mix,out} - \Delta\dot{S}_{mix,in} \end{aligned} \tag{A.7}$$

where $\Delta\dot{S}_{mix}$ is the entropy of mixing of dry air and water vapor mixture. It should also be noted that entropy of individual components ($s_{da,o}$, $s_{da,i}$, $s_{v,o}$, and $s_{v,i}$) are all evaluated at the respective moist air temperature and total pressure. A mass balance gives

$$\dot{m}_{w,i} - \dot{m}_{w,o} = \dot{m}_{da} \cdot (\omega_o - \omega_i) \tag{A.8}$$

This further reduces Eqn. A.7 to give

$$\begin{aligned} \dot{S}_{gen} &= \dot{m}_{w,i} \cdot (s_{w,o} - s_{w,i}) - \dot{m}_{da} \cdot (\omega_o - \omega_i) \cdot (s_{w,o} - s_{v,o}) \\ &\quad + \dot{m}_{da} \cdot (s_{da,o} - s_{da,i}) + \dot{m}_{da} \cdot \omega_i \cdot (s_{v,o} - s_{v,i}) \\ &\quad + \Delta\dot{S}_{mix,out} - \Delta\dot{S}_{mix,in} \end{aligned} \tag{A.9}$$

Water is assumed as an incompressible fluid, and the total pressure of the system is taken to be uniform. Assuming that dry air and water vapor exhibit ideal gas behavior, we have:

$$\begin{aligned}
\dot{S}_{gen} &= \dot{m}_{w,i} \cdot \left[c_{p,w} \cdot \ln\left(\frac{T_{w,o}}{T_{w,i}}\right)\right] \\
&\quad -\dot{m}_{da} \cdot (\omega_o - \omega_i) \cdot \left[c_{p,v} \cdot \ln\left(\frac{T_{w,o}}{T_{a,o}}\right)\right] \\
&\quad +\dot{m}_{da} \cdot (\omega_o - \omega_i) \cdot \left[R_w \cdot \ln\left(\frac{P_{sat,w,o}}{P_{total}}\right) + s_{fg,o}\right] \\
&\quad +\dot{m}_{da} \cdot c_{p,da} \cdot \ln\left(\frac{T_{a,o}}{T_{a,i}}\right) \\
&\quad +\dot{m}_{da} \cdot \omega_i \cdot c_{p,v} \cdot \ln\left(\frac{T_{a,o}}{T_{a,i}}\right) \\
&\quad +\Delta\dot{S}_{mix,out} - \Delta\dot{S}_{mix,in} \qquad \text{(A.10)}
\end{aligned}$$

where, $P_{sat,w,o}$ is the saturation pressure of water at $T_{w,o}$ and $s_{fg,o}$ is the enthalpy change of vaporization at $T_{w,o}$. The entropy of mixing for an ideal mixture can be written as:

$$\begin{aligned}
\Delta\dot{S}_{mix,out} - \Delta\dot{S}_{mix,in} &= -R_{da} \cdot \dot{m}_{da} \cdot \ln(x_{da,o}) \\
&\quad -R_w \cdot \dot{m}_{v,o} \cdot \ln(x_{v,o}) \\
&\quad +R_{da} \cdot \dot{m}_{da} \cdot \ln(x_{da,i}) \\
&\quad +R_w \cdot \dot{m}_{v,i} \cdot \ln(x_{v,i}) \qquad \text{(A.11)}
\end{aligned}$$

Here the mole fraction of dry air and water vapor can be expressed in terms of humidity ratio, ω, as:

$$\begin{aligned}
\frac{1 - x_{da}}{x_{da}} &= \frac{M_{da}}{M_v} \cdot \omega \\
&= 1.608 \cdot \omega \qquad \text{(A.12)} \\
x_{da} &= \frac{1}{1 + 1.608 \cdot \omega} \qquad \text{(A.13)} \\
x_v &= \frac{1.608 \cdot \omega}{1 + 1.608 \cdot \omega} \qquad \text{(A.14)}
\end{aligned}$$

Using these expressions for mole fraction in Eqn. A.10 we get the following.

$$\begin{aligned}
\Delta\dot{S}_{mix,out} - \Delta\dot{S}_{mix,in} &= \dot{m}_{da}\Bigg\{ R_{da} \cdot \ln\left(\frac{1 + 1.608 \cdot \omega_o}{1 + 1.608 \cdot \omega_i}\right) \\
&\quad -R_w \cdot \omega_o \cdot \ln\left(1 + \frac{1}{1.608 \cdot \omega_o}\right) \\
&\quad +R_w \cdot \omega_i \cdot \ln\left(1 + \frac{1}{1.608 \cdot \omega_i}\right) \Bigg\} \qquad \text{(A.15)}
\end{aligned}$$

Using Eqns. A.10 and A.15, we obtain Eqn. 24.